



UNIVERSITAT
POLITÈCNICA
DE VALÈNCIA



UNIVERSITAT POLITÈCNICA DE VALÈNCIA

School of Industrial Engineering

ANALYSIS OF SHADOWING EFFECT ON PHOTOVOLTAIC
PANELS ON PARALLEL VERTICAL DISTRIBUTION

End of Degree Project

Bachelor's Degree in Industrial Engineering

AUTOR/A: Mata Horrillo, Jaume Marc

Tutor/a: Giner Bosch, Vicent External cotutor: Regucki, Pawel

CURSO ACADÉMICO: 2023/2024



Wrocław University
of Science and Technology

**Faculty of Mechanical and
Power Engineering**

ANALYSIS OF SHADOWING EFFECT ON PHOTOVOLTAIC PANELS ON PARALLEL VERTICAL DISTRIBUTION

Erasmus Bachelor Thesis

Project supervisor: Paweł Regucki

Jaume Marc Mata Horrillo

ID: 283237

Index

- 1. Abstract.....2
- 2. Project Motivation3
- 3. Panel distribution4
- 4. Solar trajectory and orientation in the model5
 - 4.1 Optimal orientation, β 5
 - 4.2 Description of solar trajectory7
- 5. Irradiance Data12
- 6. Model of Shadowing14
 - 6.1 Model for direct Irradiance.14
 - 6.1.1 Mathematical foundations for direct irradiance14
 - 6.1.2 Procedure for direct irradiance model.....19
 - 6.2 Model for Indirect Irradiance.28
 - 6.2.1 Mathematical foundations for indirect irradiance29
 - 6.2.2 Procedure for indirect irradiance model35
 - 6.3 Model for Global Irradiance.41
- 7. Conclusions.....44
- 8. References45

1. Abstract

The project consists of analyzing the efficiency of photovoltaic plants with vertical distribution where panels are placed directly above each other at a certain distance. The objective of this type of installation is optimizing space to provide power for domestic buildings and small industries that need to confine the complex into smaller spaces.

The project proposes a generalist model to determine the energetic losses associated with the shadowing produced by the upper panels. This method allows the designer to calculate the situation of a particular installation depending on the distance between panel planes only by providing the location and dimensions of the power plant and applying the methodology to programming environment as the one exemplified.

Over the report of the project the model is applied to the case of Wroclaw to illustrate the procedure for two tilted parallel panels to verify the models correct operation. The results obtained enlighten the critical influence of the vertical distance between panels, applying a 20% reduction of power for simple panels for shorter distances, and foreseeing higher reductions for more complex installations.

Key words: photovoltaic; shadowing; radiation; irradiance ; PV installation ; modeling ; solar .

2. Project Motivation

The modeling of the shadowing effect is directly connected with the growing presence of photovoltaic installation in the modern world and the management of the terrain exploit.

Renewable energies have increased their presence in the energetic mix of production during the last decades in the search of substituting fossil fuels that contribute in global warming. Particularly the photovoltaic energy production has reached 1,000TWh worldwide and it is expected to rise to 6970TWh by 2030.

Under these circumstances, nowadays the main approach of shadowing in PV installations consists of using vast land surface and avoiding completely the effect of direct radiation. The issue with this approach is that the land used, especially in the countryside, could be given another use as agricultural terrain to compensate the demographic growth impact.

This project designs a method to evaluate the possibility of reducing the area used, obtaining more compact installation to free space. Geometrical approach has been chosen given that the nature of radiation behavior can be explained by mathematical analytics and the power provided is strictly bounded to Sun radiation.

3. Panel distribution

The main part of the model is designed parting from two single panels with the distribution of Figure 3.1. The dimensions of said panels would be l for length, w for width, β for angular inclination of the panel over the horizontal and h for vertical distance between panels. The parameter h will be the main dimensional value to modify in order to analyze different scenarios.

The installation towards the analysis is oriented is similar to Figure 3.2:

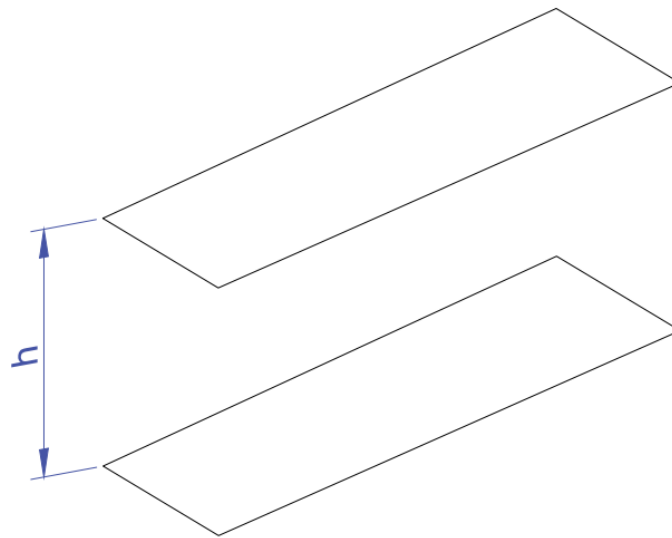


FIGURE 3.1. PANEL DISTRIBUTION

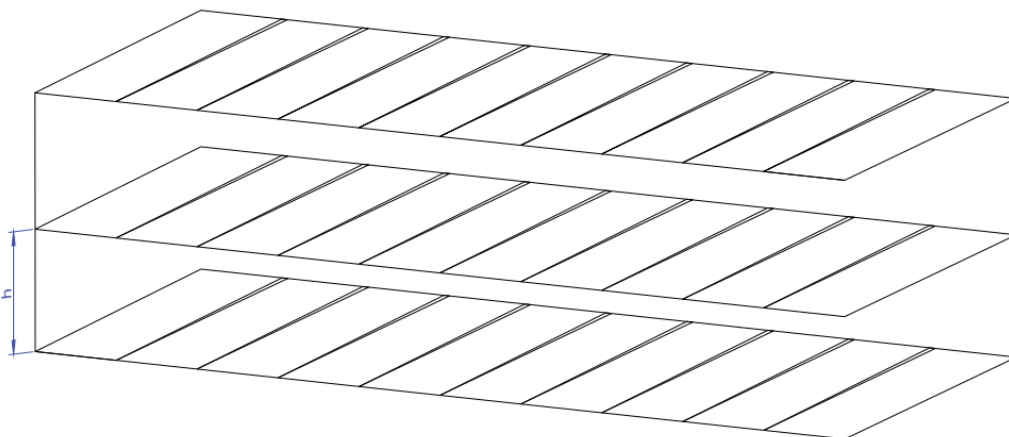


FIGURE 3.2. PV INSTALLATION DISTRIBUTION

4. Solar trajectory and orientation in the model

To depict the projection of the shadow and the optimal orientation of the panels, first it is mandatory to describe the position and trajectory of the Sun in general terms, and then, applied to the exact geographical location, in the given example, Wrocław.

4.1 Optimal orientation, β

The first step consists of selecting the optimal inclination β of the panel over the ground to accomplish maximum power.

The maximum efficiency would be accomplished with an angle of 90° between the surface of the panel and the line to the center of the Sun, an angle of incidence $\alpha=90^\circ$, since the perpendicular projection of the surface towards the Sun rays will be maximized.

However, for determining the angle of incidence correctly, the latitude where the panel is installed (angular variation from the equator) and the solar declination δ shall be considered.

$$\delta = 23,45 \cdot \sin\left(\frac{360}{365} \cdot (284 + N)\right) \quad (4.1)$$

Solar declination δ is conceived as the angular displacement of the sun's center above or below the Earth's equator, which changes depending on the day of the year as shown in Figure 4.1 due to the inclination of Earth's axis following the equation (4.1).

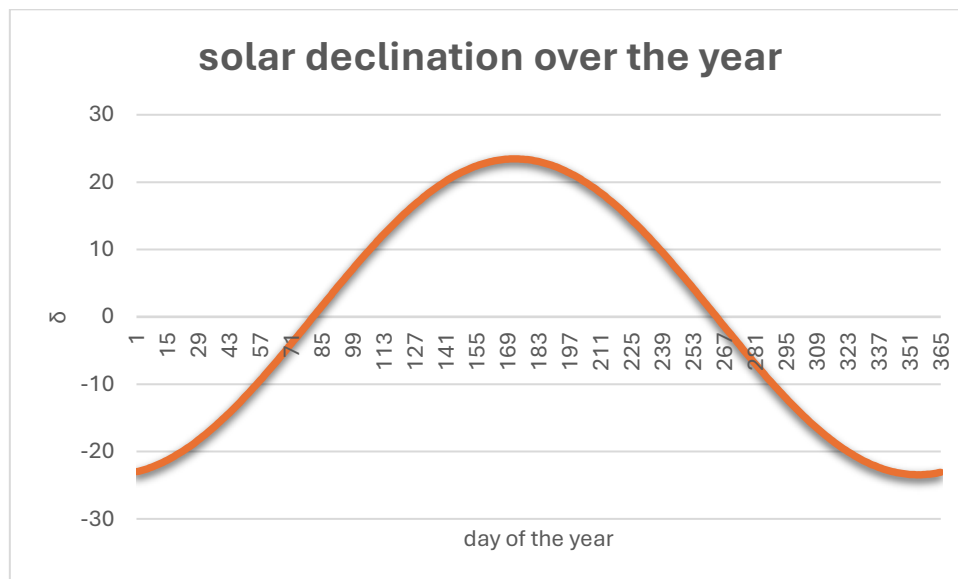


FIGURE 4.1. SOLAR DECLINATION

The criteria for choosing the δ used of the model is taking the value for the longest day of the year, which corresponds to the summer solstice, Figure, N = 172 ,21st of June, with $\delta=23,45^\circ$.

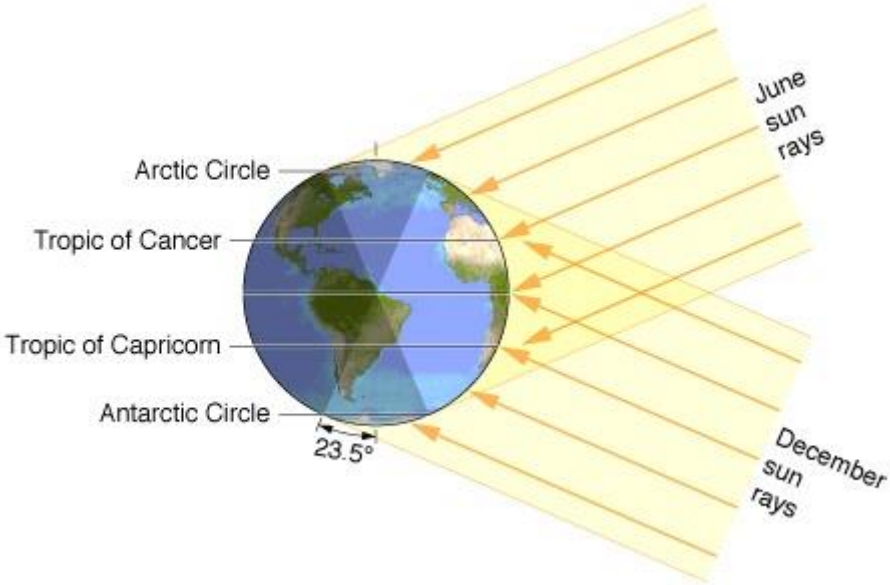


FIGURE 4.2. PROVIDED BY WEBER STATE UNIVERSITY [13]

Therefore, the max angle of incidence can be calculated as:

$$\alpha_{max} = 90 - lat + \delta \tag{4.2}$$

And the inclination of the panel from the ground β :

$$\beta = 90 - \alpha_{max} \tag{4.3}$$

Figure 4.3 and Figure 4.4 illustrate the cases for the summer solstice and the winter solstice:

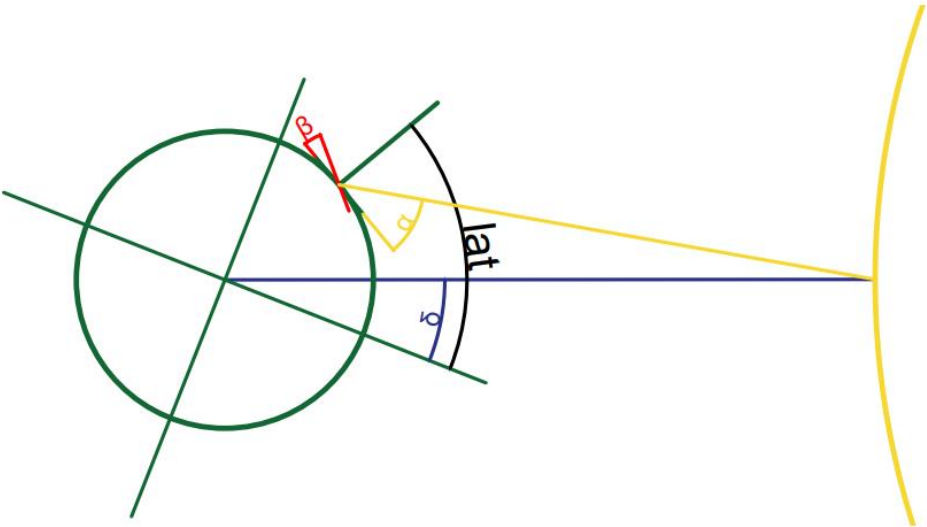


FIGURE 4.3. SUMMER SOLSTICE

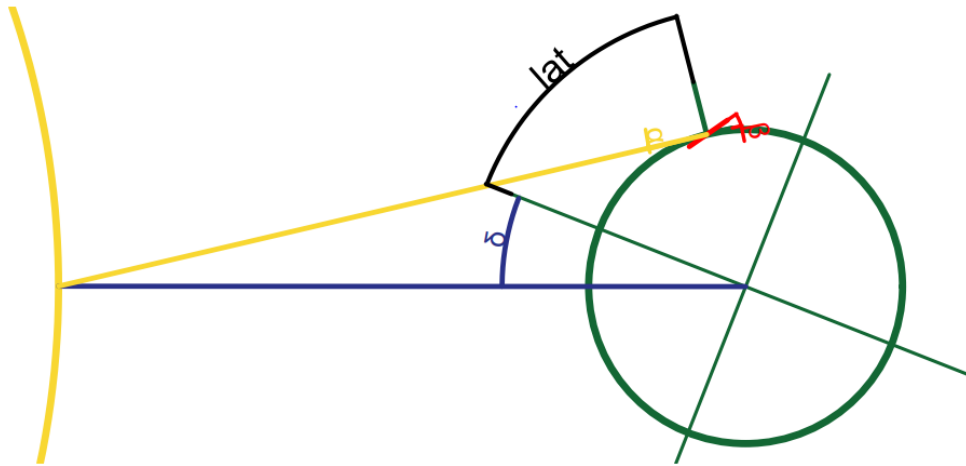


FIGURE 4.4. WINTER SOLSTICE

The result obtained following that formula for the location on the study is presented in Table 4.1:

TABLE 4.1 GEOMETRICAL PARAMETERS FOR WROCLAW

	latitude	α	β	degrees over equator
Wroclaw	51,1 N	62,3°	27,7°	51,1°

The values over the equator are important because they are needed for checking at the PHOTOVOLTAIC GEOGRAPHICAL INFORMATION SYSTEM (PGIS) of the European Commission for monthly data [1].

4.2 Description of solar trajectory

Determining the solar trajectory is crucial for the model since it provides the coordinates for each Sun position. Those coordinates are used in the model to describe mathematically the direction of Sun rays, and, consequently, the area of the panel directly shadowed.

The trajectory of the Sun seen from a certain point can be presented in polar coordinates with the denominated angles Azimuth γ for horizontal plane and the already presented α for vertical plane, α can be referred as elevation angle too.

As explained before, the declination angle changes over the year so instead of a singular trajectory, we have a spectrum of trajectories contained between the solstices as shown in Figure 4.5. Each trajectory

has been discretized into one fixed position for each hour of the day. The number of days calculated is reduced also to one day per month which represents the average conditions for the entire month.

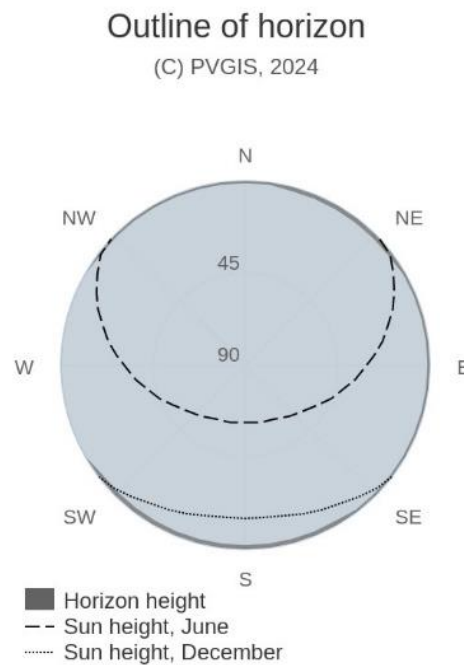


FIGURE 4.5. LIMITS OF TRAJECTORY SPECTRUM IN WROCLAW PROVIDED BY THE PHOTOVOLTAIC GEOGRAPHICAL INFORMATION SYSTEM (PGIS) OF THE EUROPEAN COMMISSION [1].

The data calculation follows advanced formulation, in this model, it is obtained by Image Circuits [10] spreadsheet sunpath.xls. The spreadsheet requires coordinates of the geographical position, a selected day of the month and the magnetic variation, a characteristic value of the location.

Parameters for Wroclaw are presented in Table 4.2 and in Figure 4.6.

TABLE 4.2 GEOGRAPHICAL PARAMETERS FOR WROCLAW

Latitude	Longitude	Day of month	Magnetic variation	Local time
51° 6' N	17° 60' E	10	5,77°	+1:00 UTC



FIGURE 4.6. COORDINATES PROVIDED BY MAGNETIC.DECLINATION.COM [11]

The results for Wrocław sun path are as shown for two sample months in Table 4.3 and Table 4.4:

TABLE 4.3. 10TH OF JANUARY SOLAR PATH

	γ	α
Time	Azimuth	Elevation
4,00	-92,09	-34,91
5,00	-80,22	-25,51
6,00	-69,12	-16,23
7,00	-58,13	-7,40
8,00	-46,73	0,97
9,00	-34,59	7,50
10,00	-21,51	12,70
11,00	-7,57	15,96
12,00	6,88	16,96
13,00	21,30	15,61
14,00	35,13	12,04
15,00	48,06	6,59
16,00	60,09	0,01
17,00	71,40	-8,67
18,00	82,39	-17,58
19,00	93,57	-26,89
20,00	105,66	-36,27

TABLE 4.4.10TH OF FEBRUARY SOLAR PATH

	γ	α
Time	Azimuth	Elevation
4,00	-99,39	-30,27
5,00	-86,99	-20,96
6,00	-75,45	-11,55
7,00	-64,04	-2,33
8,00	-52,22	6,14
9,00	-39,53	13,46
10,00	-25,67	19,29
11,00	-10,64	23,12
12,00	5,17	24,53
13,00	21,01	23,34
14,00	36,13	19,71
15,00	50,10	14,03
16,00	62,90	6,81
17,00	74,79	-1,49
18,00	86,23	-10,72
19,00	97,76	-20,11
20,00	110,09	-29,41

The charts for the whole data are represented in the following Figure 4.7 and Figure 4.8:

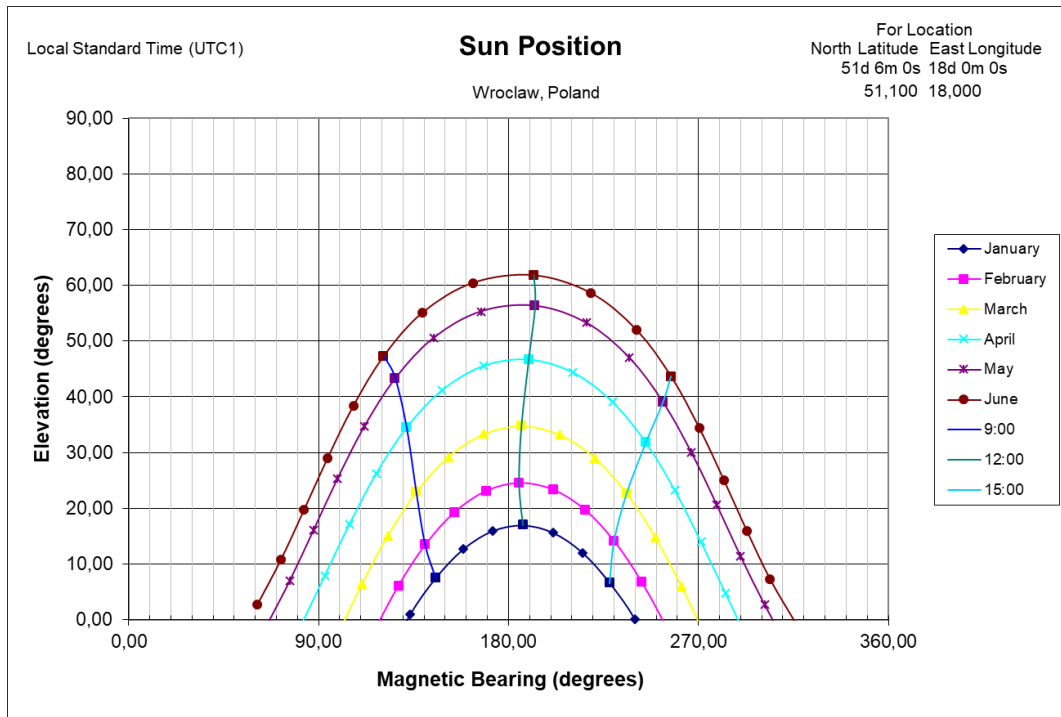


FIGURE 4.7. PROVIDED BY IMAGINE CIRCUITS [10]

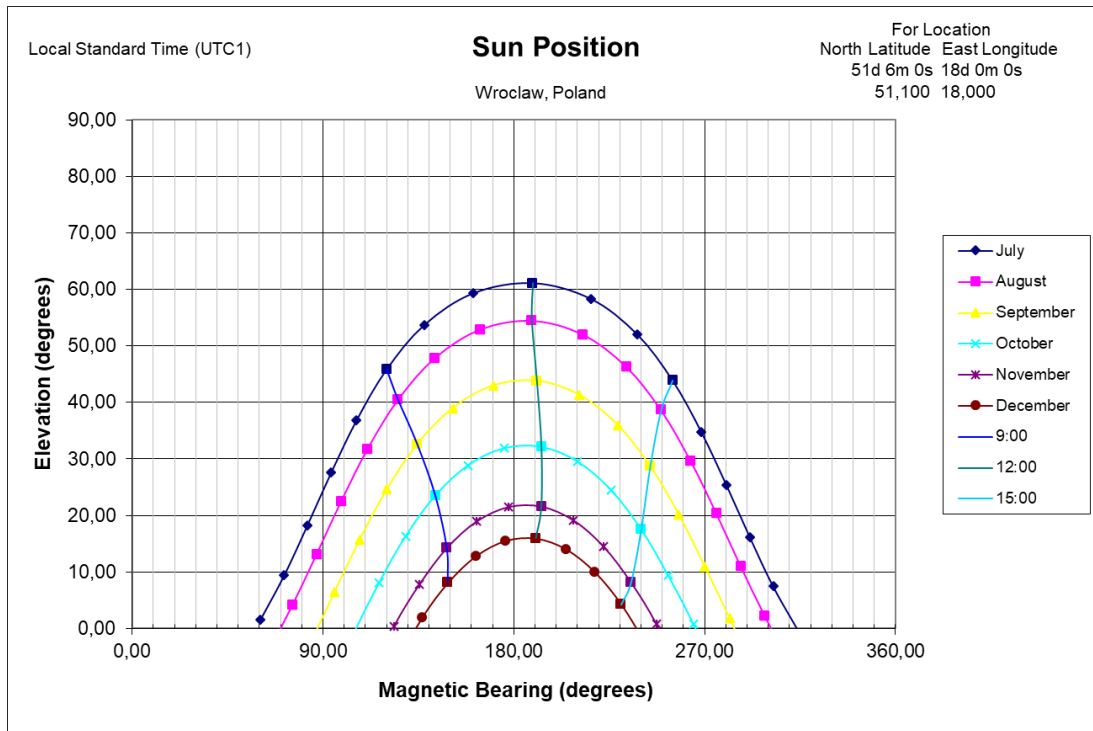


FIGURE 4.8. PROVIDED BY IMAGINE CIRCUITS [10]

The figures Figure 4.7 and Figure 4.8 show that the best results, higher elevations, are accomplished with a South orientation, $\gamma=0$. Also, we can confirm the model in the Imagine Circuits file is suitable for finding α since the program has given us a max height α of 61 degrees, a relative error inferior to 2% towards the official data provided by PHOTOVOLTAIC GEOGRAPHICAL INFORMATION SYSTEM (PGIS) of the European Commission [1].

5. Irradiance Data

Solar radiation energy suffers significant reductions in its entering into Earth's atmosphere. Around 25% of it is reflected in the upper layers of atmosphere. The entering radiation is divided into direct radiation, diffuse radiation and reflected radiation as exemplified in

Also, the concept of irradiance $G_{\frac{1}{m^2}} [kW/m^2]$ defines the power of the radiation passing through per square meter of surface irradiated. This parameter will be the decisive indicator to relate the power production of the installation with its dimensions. Irradiance is divided into direct irradiance, indirect irradiance and reflected irradiance, depending on the type of radiation.

Direct radiation is the percentage of radiation that gets from the Sun to the surface without being reflected or absorbed at any layer of the atmosphere. Direct irradiance $G_{\frac{b}{m^2}}$ represents most of the radiation on clear sky days and its utilization on photovoltaic highly depends on avoiding objects intercepting sun rays.

Diffuse radiation includes all the radiation spread by gas molecules on air and suspended particles. Indirect irradiance $G_{\frac{d}{m^2}}$ is associated with diffuse radiation and represents bigger percentages on cloudy weather. When equal distribution of light on the environment is assumed, indirect irradiance reduction will strongly depend on the proximity of objects surrounding the photovoltaic cell.

Reflected radiation and irradiance are the smallest portion of sun radiation and represent the rest of it that is not absorbed but reflected on Earth's surface. Due to its small value, the model presented neglects the reduction of it caused by the installation configuration.

Finally, the information intended to achieve is the multiplication of irradiance per area irradiated, also known as irradiation $G [kW]$.

The model for panels above each other bases the final energy received on the standard values of irradiance for the selected geographical location.

In the case of Europe, those values are provided by the PHOTOVOLTAIC GEOGRAPHICAL INFORMATION SYSTEM (PGIS) of the European Commission [1] and can be downloaded for every hour of a representative day of the month by selecting daily data. Is important to point out that the β introduced in the system shall be the one over the equator, not over the horizon as calculated in equation (4.1).

In the case of Wroclaw, the data for 27° (51° in the system) are as the one in the example Table 5.1:

TABLE 5.1 IRRADIANCE DATA FOR 10TH OF JANUARY

Results for: January			
Slope of plane (deg.):			52
Azimuth (orientation) of plane (deg.):			0
time (UTC+1)	G(i)	Gb(i)	Gd(i)
0:00	0.0	0.0	0.0
1:00	0.0	0.0	0.0
2:00	0.0	0.0	0.0
3:00	0.0	0.0	0.0
4:00	0.0	0.0	0.0
5:00	0.0	0.0	0.0
6:00	0.0	0.0	0.0
7:00	0.0	0.0	0.0
8:00	28.74	21.24	7.16
9:00	175.78	109.15	63.7
10:00	237.63	142.74	90.21
11:00	270.76	162.7	102.47
12:00	276.97	165.78	105.39
13:00	264.62	162.16	97.18
14:00	203.73	123.34	76.52
15:00	132.21	86.11	44.11
16:00	1.51	0.69	0.78
17:00	0.0	0.0	0.0
18:00	0.0	0.0	0.0
19:00	0.0	0.0	0.0
20:00	0.0	0.0	0.0
21:00	0.0	0.0	0.0
22:00	0.0	0.0	0.0
23:00	0.0	0.0	0.0

6. Model of Shadowing

The model of the Shadowing effect is divided into two sub models for direct and indirect irradiance even they share parameters and can be applied in the same programming workspace. Along chapter 6 these sub models will be described and exemplified with a programming proposal for them.

6.1 Model for direct Irradiance.

Direct Irradiance model focuses on detecting which sectors of the panel are shadowed at any time to apply the proportional irradiated area reduction.

6.1.1 Mathematical foundations for direct irradiance

Since the direct shading is associated with a geometrical problem, the matter shall be approached geometrically.

The model here described returns the area directly irradiated of the panel for any moment of the year and, consequently, the energy received and the percentual reduction of the direct radiance based on the following variables:

- Dimensions and configuration of the panel or installation, l , w and β .
- Location of the installation, Sun trajectory (α , γ) and Irradiance data depend on the geographical location.
- Range of distances between panel planes, separated vertically by height h .

By contrast, the model as defined has some restrictions such as:

- South orientation of the panels is imposed. It could though be modified by adding a $\Delta\gamma$ according to the number of degrees turned from south orientation to every value of γ for the sun path.
- Parallelism between panels can't be changed.
- Discretization of nodes is limited; therefore, the area is approximated.
- Opacity of the objects is assumed.

Firstly, it is defined the center of cartesian coordinates in 3D and the location of the corners of the upper panel. The point corresponding to the corner A it is taken for the origin. Thus, for a panel with dimensions $l \times w$ and an inclination β the points result as in expression (6.1).

$$A = \begin{pmatrix} 0 \\ 0 \\ 0 \end{pmatrix} \quad B = \begin{pmatrix} 0 \\ w \\ 0 \end{pmatrix} \quad C = \begin{pmatrix} l \cdot \cos(\beta) \\ 0 \\ l \cdot \sin(\beta) \end{pmatrix} \quad D = \begin{pmatrix} l \cdot \cos(\beta) \\ w \\ l \cdot \sin(\beta) \end{pmatrix} \quad (6.1)$$

Secondly, to find the shadow projected on the lower panel plane, the intersection between the straight line corresponding to the sunlight that passes through each corner and the given plane π must be formulated.

Plane π_0 is given by the point P_{π_0} , two vectors \vec{v} , \vec{u} and two constant values, μ and σ as in (6.2)(6.3)(6.4)(6.5).

$$P_{\pi_0} = \begin{pmatrix} 0 \\ 0 \\ -h \end{pmatrix} \quad (6.2)$$

$$\vec{v} = \begin{pmatrix} 0 \\ 1 \\ 0 \end{pmatrix} \quad (6.3)$$

$$\vec{u} = \begin{pmatrix} \cos(\beta) \\ 0 \\ \sin(\beta) \end{pmatrix} \quad (6.4)$$

$$\pi_0: \quad \begin{pmatrix} x \\ y \\ z \end{pmatrix} = \begin{pmatrix} 0 \\ 0 \\ -h \end{pmatrix} + \mu \cdot \begin{pmatrix} 0 \\ 1 \\ 0 \end{pmatrix} + \sigma \cdot \begin{pmatrix} \cos(\beta) \\ 0 \\ \sin(\beta) \end{pmatrix} \quad (6.5)$$

Sunlight rays' straight line is given by any of the previous defined points A, B, C and D generalized as X_{ir} , the vector \vec{w} , (6.6), and a constant k as in (6.6).

$$\vec{w} = \begin{pmatrix} \cos(\alpha) \cos(\gamma) \\ -\cos(\alpha) \sin(\gamma) \\ -\sin(\alpha) \end{pmatrix} \quad (6.6)$$

Note that \vec{w} is a function of (α) and (γ) depending on the position of the Sun, providing the limits of the shadow for any moment of the year and day.

$$r_i: \begin{pmatrix} x \\ y \\ z \end{pmatrix} = \begin{pmatrix} x_{ir} \\ y_{ir} \\ z_{ir} \end{pmatrix} + k \cdot \begin{pmatrix} \cos(\alpha) \cos(\gamma) \\ -\cos(\alpha) \sin(\gamma) \\ -\sin(\alpha) \end{pmatrix} \quad (6.7)$$

The intersection of each r_i result on equation (6.8):

$$k = \frac{-\sin \beta \cdot x_{ir} + \cos \beta \cdot (z_{ir} + h)}{\sin \beta \cos \alpha \cos \gamma + \cos \beta \sin \alpha} \quad (6.8)$$

Therefore, any point shadowed is given by the expression (6.9) and exemplified in Figure 6.1:

$$\begin{pmatrix} x \\ y \\ z \end{pmatrix} = \begin{pmatrix} x_{ir} \\ y_{ir} \\ z_{ir} \end{pmatrix} + \frac{-\sin \beta \cdot x_{ir} + \cos \beta \cdot (z_{ir} + h)}{\sin \beta \cos \alpha \cos \gamma + \cos \beta \sin \alpha} \cdot \begin{pmatrix} \cos(\alpha) \cos(\gamma) \\ -\cos(\alpha) \sin(\gamma) \\ -\sin(\alpha) \end{pmatrix} \quad (6.9)$$

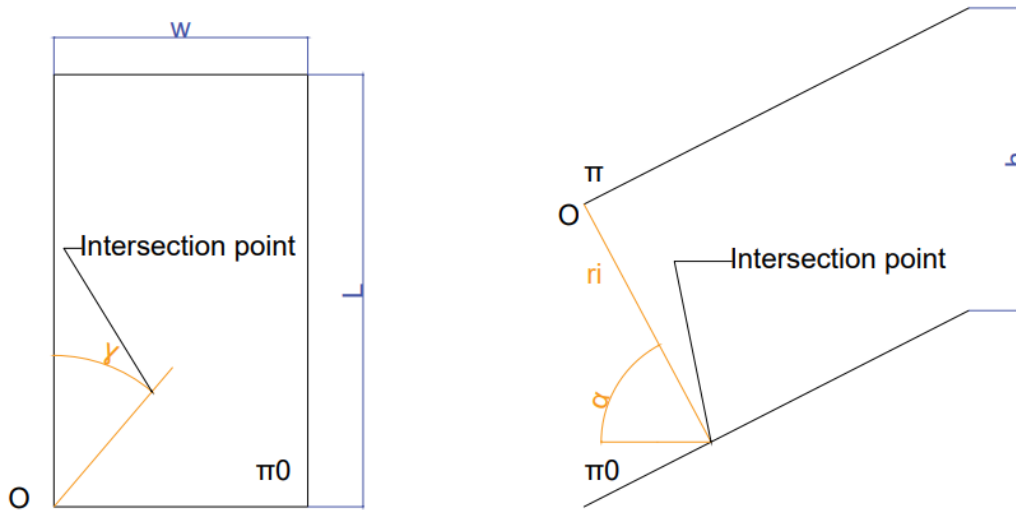


FIGURE 6.1. INTERSECTION POINT

This process can be repeated in any program or worksheet for points following the side contour of the upper panel, spacing in t fractions of l as in (6.10), Δl_r from A to C and from B to D, to get the borders of the shadow.

$$\Delta l_r = \frac{l}{t} \quad (6.10)$$

The borders X_{ir} are discretized into points with the following equations (6.11)(6.12):

$$X_{ir} = \begin{pmatrix} x \\ y \\ z \end{pmatrix} = \begin{pmatrix} i \cdot \Delta l_r \cdot \cos(\beta) \\ 0 \\ -h + i \cdot \Delta l \cdot \sin(\beta) \end{pmatrix} \quad i \in (0, t); \quad (6.11)$$

$$X_{ir} = \begin{pmatrix} x \\ y \\ z \end{pmatrix} = \begin{pmatrix} i \cdot \Delta l_r \cdot \cos(\beta) \\ w \\ -h + i \cdot \Delta l \cdot \sin(\beta) \end{pmatrix} \quad i \in (0, t); \quad (6.12)$$

It's observed that both lines are parallel in the shadow to the original lines of the panel so it can be determined the maximum and minimum value for x and y , and assign them to (6.13).

$$x_{max}, x_{min}, y_{max}, y_{min} \quad (6.13)$$

On the other hand, it is possible to define the points of the plane occupied by the lower panel the same way done for the upper panel with a vertical translation given by the value h as the points in (6.14).

$$AA = \begin{pmatrix} 0 \\ 0 \\ -h \end{pmatrix} \quad BB = \begin{pmatrix} 0 \\ w \\ -h \end{pmatrix} \quad CC = \begin{pmatrix} l \cos(\beta) \\ 0 \\ -h + l \sin(\beta) \end{pmatrix} \quad DD = \begin{pmatrix} l \cos(\beta) \\ w \\ -h + l \sin(\beta) \end{pmatrix} \quad (6.14)$$

A proper meshing of the lower panel is accomplished discretizing it in nodes separated a distance Δl dividing l in q parts, (6.15), in x-axis and a Δw dividing w in s parts, (6.16), in y-axis.

$$\Delta l = \frac{l}{q} \quad (6.15)$$

$$\Delta w = \frac{w}{s} \quad (6.16)$$

Every node responds to equation (6.17) resulting on Figure 6.2:

$$\begin{pmatrix} x \\ y \\ z \end{pmatrix} = \begin{pmatrix} i \cdot \Delta l \cdot \cos(\beta) \\ j \cdot \Delta w \\ -h + i \cdot \Delta l \cdot \sin(\beta) \end{pmatrix} \quad i \in (0, q); j \in (0, s) \quad (6.17)$$

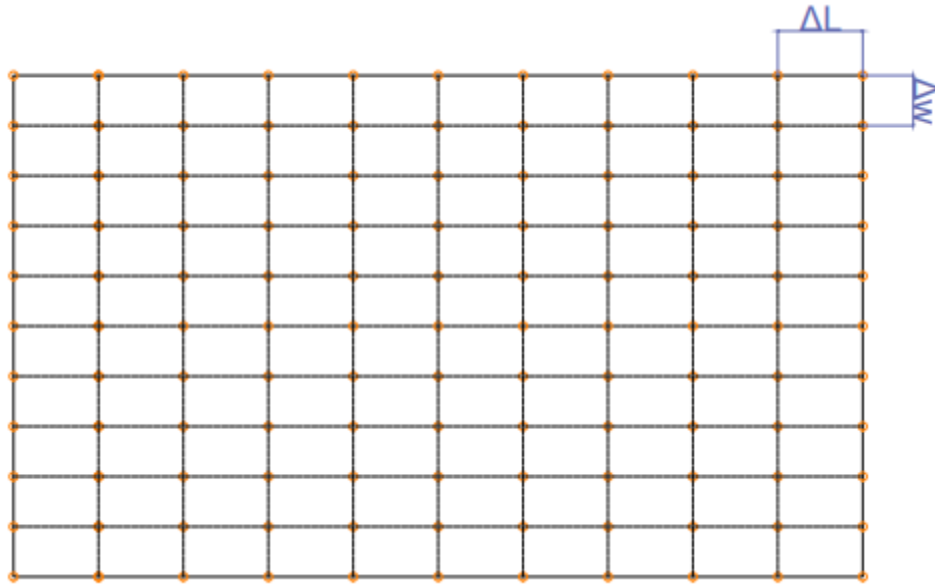


FIGURE 6.2. NODE & SECTOR DISTRIBUTION

Finally, checking the nodes on the panel with the limits of the shadow follows the condition(6.18):

(6.18)

If x is between x_{max} and x_{min} and y between y_{max} and y_{min} simultaneously , then the node is considered shadowed.

Repeating the process for every node the number of nodes shadowed is obtained.

In order to get the Area shadowed, each node is assigned a surface based on the area surrounding it:

- The nodes in the center of the panel get a rectangle of Δl per a Δw as (6.19):

$$A_c = \Delta l \cdot l \cdot \Delta w \cdot w \quad (6.19)$$

- The nodes in the sides get half the area of the central nodes as (6.20):

$$A_s = \frac{1}{2} \cdot A_c \quad (6.20)$$

- The nodes in the corner get one quarter of the area of the central nodes as (6.21):

$$A_{cr} = \frac{1}{4} \cdot A_c \quad (6.21)$$

The sum of the areas of the nodes, sectors, not categorized as shadowed gives the area irradiated A_i in (6.23):

$$A_i = n \cdot A_c + m \cdot A_s + p \cdot A_{cr} \quad (6.22)$$

- The constants n, m, p correspond to the number of sectors irradiated of each kind.

The percentage of the total area and power exploited for the given conditions is expressed as equation (6.23):

$$\%A_i = \frac{A_i}{l \cdot w} \quad (6.23)$$

Finally, the power supplied G_b , direct irradiation, can be obtained multiplying the area irradiated A_i by the direct irradiance per meter G_b/m as (6.24):

$$G_b = A_i \cdot G_b/m \quad (6.24)$$

5.1.2 Procedure for direct irradiance model

The application of the model described into computer programming for several h values permit to study the impact of the shadowing depending on the distance between panels.

The tool proposed in this thesis is Microsoft Excel since it is one of the most used and known software by engineers. The procedure for the example in Wroclaw has been programmed in an Excel worksheet.

At first, Δl , Δw and Δl_r must be determined to configure the worksheet accordingly. Equations (6.10)(6.15)(6.16) are used for selecting q , s and t . The values q , s and t are chosen by the user of the model. The recommendation is using bigger fractions for bigger dimensions of the installation. In the case of a single panel the model has been configured with:

$$q = 10; \Delta l = 0,1$$

$$s = 20; \Delta w = 0,05$$

$$t = 10; \Delta l_r = 0,1$$

The number of tables programmed on the sheet and their dimensions depend on these variables. From now on, the rest of the parameters can be easily changed just by modifying their assigned cell.

The fixed parameters needed to run the model are l , w , β and the range of values for h , Δh . The angle β is calculated by equations (4.2)(4.3). The range Δh is recommended to start at least at $h=1$ to leave enough space for installation and end at the h where the shadow has no impact anymore. Example of parameters in Wroclaw shown in Table 6.1 and Table 6.2. The dimensions $l \times w$ of the panel are the standard ones for a 60-cell domestic panel.

TABLE 6.1. Δh CHOSEN

h	1	1,25	1,5	1,75	2	2,25	2,5	2,75	3	3,25	3,5
----------	---	------	-----	------	---	------	-----	------	---	------	-----

TABLE 6.2. DIMENSION PARAMETERS

length	width	β	senβ	cosβ
1,7	1	27,7	0,46	0,89

The sun path coordinates α and γ for the location explained in point 4.2 are added to the model and the direct irradiance data explained in point 5 too as in Table 4.3 and Table 5.1 but for every value.

From this point a loop must be programmed, the following operations of the model will be repeated for each h in Δh and for each (γ, α) corresponding to each hour from 4:00 to 20:00 for the given day for each month.

With the parameters selected and for each h , the planes π and π_0 are described as in (6.5), the contour points are determined by (6.11)(6.12) and the node meshing coordinates obtained by (6.17)

For Wroclaw the meshing coordinates for $h = 3,5$ are according to Table 6.3 and Table 6.4 ,covering the range of i in equation (6.17). This results on q tables with s rows each.

TABLE 6.3. MESHING NODES FIXING Y=0%

Iteration in X_axis	X_node	Y_node	Z_node
0· l	0,00	0,00	-3,50
0,05· l	0,08	0,00	-3,46
0,1· l	0,15	0,00	-3,42
0,15· l	0,23	0,00	-3,38
0,2· l	0,30	0,00	-3,34
0,25· l	0,38	0,00	-3,30
0,3· l	0,45	0,00	-3,26
0,35· l	0,53	0,00	-3,22
0,4· l	0,60	0,00	-3,18
0,45· l	0,68	0,00	-3,14
0,5· l	0,75	0,00	-3,10
0,55· l	0,83	0,00	-3,07
0,6· l	0,90	0,00	-3,03
0,65· l	0,98	0,00	-2,99
0,7· l	1,05	0,00	-2,95
0,75· l	1,13	0,00	-2,91
0,8· l	1,20	0,00	-2,87
0,85· l	1,28	0,00	-2,83
0,9· l	1,35	0,00	-2,79
0,95· l	1,43	0,00	-2,75
1· l	1,51	0,00	-2,71

TABLE 6.4. MESHING NODES FIXING Y=10%

Iteration in X_axis	X_node	Y_node	Z_node
0· l	0,00	0,10	-3,50
0,05· l	0,08	0,10	-3,46
0,1· l	0,15	0,10	-3,42
0,15· l	0,23	0,10	-3,38
0,2· l	0,30	0,10	-3,34
0,25· l	0,38	0,10	-3,30
0,3· l	0,45	0,10	-3,26
0,35· l	0,53	0,10	-3,22
0,4· l	0,60	0,10	-3,18
0,45· l	0,68	0,10	-3,14
0,5· l	0,75	0,10	-3,10
0,55· l	0,83	0,10	-3,07
0,6· l	0,90	0,10	-3,03
0,65· l	0,98	0,10	-2,99
0,7· l	1,05	0,10	-2,95
0,75· l	1,13	0,10	-2,91
0,8· l	1,20	0,10	-2,87
0,85· l	1,28	0,10	-2,83
0,9· l	1,35	0,10	-2,79
0,95· l	1,43	0,10	-2,75
1· l	1,51	0,10	-2,71

The equation (6.9) expresses the intersection points for the borders depicted by equations (6.11)(6.12) with the parameters already added to the model.

In the example the table for the intersection of r_i and the points of intersection with plane π_0 for $h = 2 m$ and 10th day of April at 12:00 are shown in Table 6.5.

TABLE 6.5. INTERSECTION POINTS

points	xor	yor	zor	k	x	y	z
P0-A	0,00	0,00	0,00	1,85	1,25	-0,21	-1,34
P1	0,15	0,00	0,08	1,85	1,40	-0,21	-1,27
P2	0,30	0,00	0,16	1,85	1,55	-0,21	-1,19
P3	0,45	0,00	0,24	1,85	1,70	-0,21	-1,11
P4	0,60	0,00	0,32	1,85	1,85	-0,21	-1,03
P5	0,75	0,00	0,40	1,85	2,00	-0,21	-0,95
P6	0,90	0,00	0,47	1,85	2,15	-0,21	-0,87
P7	1,05	0,00	0,55	1,85	2,30	-0,21	-0,79
P8	1,20	0,00	0,63	1,85	2,45	-0,21	-0,71
P9	1,35	0,00	0,71	1,85	2,60	-0,21	-0,63
P10-B	1,51	0,00	0,79	1,85	2,75	-0,21	-0,55
P11-C	0,00	1,00	0,00	1,85	1,25	0,79	-1,34
P12	0,15	1,00	0,08	1,85	1,40	0,79	-1,27
P13	0,30	1,00	0,16	1,85	1,55	0,79	-1,19
P14	0,45	1,00	0,24	1,85	1,70	0,79	-1,11
P15	0,60	1,00	0,32	1,85	1,85	0,79	-1,03
P16	0,75	1,00	0,40	1,85	2,00	0,79	-0,95
P17	0,90	1,00	0,47	1,85	2,15	0,79	-0,87
P18	1,05	1,00	0,55	1,85	2,30	0,79	-0,79
P19	1,20	1,00	0,63	1,85	2,45	0,79	-0,71
P20	1,35	1,00	0,71	1,85	2,60	0,79	-0,63
P21-D	1,51	1,00	0,79	1,85	2,75	0,79	-0,55

Condition (6.18) is formulated with excel commands, boundaries are stored in a table such as Table 6.6 and the result of the comparison is stored as TRUE for shaded nodes for each one of them as shown in Table 6.7 for the same parameters as Table 6.5, added to lower panel tables.

TABLE 6.6. SHADOW BORDERS

	x	y
Min	1,25	-0,21
Max	2,75	0,79

TABLE 6.7. SHADOW CONDITION IN LOWER PANEL

Y=0%	x	y	z	Shade
0· l	0,00	0,00	-3,50	FALSE
0,05· l	0,08	0,00	-3,46	FALSE
0,1· l	0,15	0,00	-3,42	FALSE
0,15· l	0,23	0,00	-3,38	FALSE
0,2· l	0,30	0,00	-3,34	FALSE
0,25· l	0,38	0,00	-3,30	FALSE
0,3· l	0,45	0,00	-3,26	FALSE
0,35· l	0,53	0,00	-3,22	FALSE
0,4· l	0,60	0,00	-3,18	FALSE
0,45· l	0,68	0,00	-3,14	FALSE
0,5· l	0,75	0,00	-3,10	FALSE
0,55· l	0,83	0,00	-3,07	FALSE
0,6· l	0,90	0,00	-3,03	FALSE
0,65· l	0,98	0,00	-2,99	FALSE
0,7· l	1,05	0,00	-2,95	FALSE
0,75· l	1,13	0,00	-2,91	FALSE
0,8· l	1,20	0,00	-2,87	FALSE
0,85· l	1,28	0,00	-2,83	TRUE
0,9· l	1,35	0,00	-2,79	TRUE
0,95· l	1,43	0,00	-2,75	TRUE
1· l	1,51	0,00	-2,71	TRUE

The proposed model in Excel offers the possibility to represent graphically the shading situation of the panel by referring the cells with the logical values of condition into a rearranged distribution with the panel shape.

Figures Figure 6.3, Figure 6.4, Figure 6.5 and Figure 6.6 illustrate the result of the rearranged distribution for 10th of August at 10:00, 11:00, 12:00 and 15:00 to observe the movement of the shadow inwards at 10:00 and 11:00 and leaving the panel from 12:00 to 15:00

The number of nodes, representing sectors of the panel, are summed up and the equations (6.19)(6.20)(6.21) (6.22) are used to calculate the area shaded per sector as shown in Table 6.8 and Table 6.9.

TABLE 6.8. SECTORS IRRADIATED

Sectors	Area of a Sector in XY (cm^2)	Area of a Sector in panel plane (cm^2)
75	75,2	85,0
36	37,6	42,5
3	18,8	21,3

TABLE 6.9. TOTAL AREA IRRADIATED

Area Irradiated
0,79688 m^2

Equations (6.23)(6.24) calculate the percentage of area radiated and the direct irradiation resultant.

The loop will repeat this process, changing h and sun's position coordinates values and storing the Enlighted area resulting for each set of conditions.

The example has been programmed with a Macro in Excel, in TypeScript language, which executes a for loop, with the explained sun path and Δh limits, copying the values from the cells with the set of conditions into the variable parameter cells and then copying back the area result into the column of results. This macro can be linked to the excel worksheet, resulting in a worksheet that only needs l, w, β a range of h and running the macro to automatically receive the direct irradiation received in shadowing conditions.

The Table 6.10 present the result tables at excel for $h = 1$ and $h = 1,25$ In May and June, showing the percentage of panel area directly irradiated and then direct irradiation received.

TABLE 6.10 .DIRECT IRRADIATION 10TH OF MAY & 10TH OF JUNE

H=			1,00				1,25			
	gamma	alpha	Area	Area%	Gb/m(i)	Gb(i)	Area	Area%	Gb/m(i)	Gb(i)
Time	Az	Elev								
4,00	-115,27	-1,51	1,70	100,00	0,00	0,00	1,70	100,00	0,00	0,00
5,00	-103,75	6,94	1,70	100,00	0,00	0,00	1,70	100,00	0,00	0,00
6,00	-92,52	16,01	1,70	100,00	19,11	32,49	1,70	100,00	19,11	32,49
7,00	-80,98	25,39	1,70	100,00	99,71	169,51	1,70	100,00	99,71	169,51
8,00	-68,38	34,66	1,70	100,00	198,66	337,72	1,70	100,00	198,66	337,72
9,00	-53,69	43,31	1,30	76,38	294,65	382,57	1,54	90,63	294,65	453,95
10,00	-35,57	50,58	0,95	56,13	354,14	337,89	1,16	68,38	354,14	411,64
11,00	-13,06	55,33	0,72	42,63	366,09	265,28	0,87	51,13	366,09	318,18
12,00	12,48	56,34	0,72	42,63	359,64	260,60	0,87	51,13	359,64	312,57
13,00	36,85	53,28	0,95	56,13	333,42	318,12	1,12	65,63	333,42	371,97
14,00	57,07	47,08	1,27	74,63	264,39	335,41	1,41	83,13	264,39	373,62
15,00	73,26	38,99	1,63	95,88	198,95	324,26	1,70	100,00	198,95	338,22
16,00	86,72	29,95	1,70	100,00	122,11	207,59	1,70	100,00	122,11	207,59
17,00	98,67	20,59	1,70	100,00	37,93	64,48	1,70	100,00	37,93	64,48
18,00	109,98	11,33	1,70	100,00	0,00	0,00	1,70	100,00	0,00	0,00
19,00	121,30	2,67	1,70	100,00	0,00	0,00	1,70	100,00	0,00	0,00
20,00	133,14	-5,54	1,70	100,00	0,00	0,00	1,70	100,00	0,00	0,00
4,00	-118,91	2,71	1,70	100,00	0,00	0,00	1,70	100,00	0,00	0,00
5,00	-107,74	10,76	1,70	100,00	0,00	0,00	1,70	100,00	0,00	0,00
6,00	-96,83	19,67	1,70	100,00	15,61	26,54	1,70	100,00	15,61	26,54
7,00	-85,65	28,99	1,70	100,00	96,41	163,90	1,70	100,00	96,41	163,90
8,00	-73,45	38,35	1,70	100,00	195,77	332,81	1,70	100,00	195,77	332,81
9,00	-59,06	47,30	1,27	74,63	275,53	349,54	1,41	83,13	275,53	389,36
10,00	-40,75	55,08	0,90	52,88	331,73	298,18	1,07	62,88	331,73	354,58
11,00	-16,73	60,45	0,65	38,38	357,23	233,05	0,80	46,88	357,23	284,67
12,00	11,94	61,80	0,53	31,13	349,74	185,06	0,72	42,63	349,74	253,43
13,00	39,16	58,59	0,90	52,88	326,11	293,13	0,95	56,13	326,11	311,15
14,00	60,64	52,01	1,11	65,13	265,03	293,42	1,39	81,88	265,03	368,89
15,00	77,05	43,63	1,63	95,63	191,20	310,82	1,70	100,00	191,20	325,04
16,00	90,34	34,44	1,70	100,00	125,60	213,52	1,70	100,00	125,60	213,52
17,00	102,01	25,05	1,70	100,00	45,77	77,81	1,70	100,00	45,77	77,81
18,00	112,99	15,87	1,70	100,00	0,00	0,00	1,70	100,00	0,00	0,00
19,00	123,95	7,26	1,70	100,00	0,00	0,00	1,70	100,00	0,00	0,00
20,00	135,36	-0,17	1,70	100,00	0,00	0,00	1,70	100,00	0,00	0,00

6.2 Model for Indirect Irradiance.

As for Indirect irradiance, the effect of the panel above is not dependent of Solar position. Diffuse radiance reduction is caused constantly based on the solid angle occupied by the upper panel, depending on the point of observation selected on the lower panel.

6.2.1 Mathematical foundations for indirect irradiance

Solid angle is defined as the amount of field of view occupied by the projection of a surface over an observation point, shown in Figure 6.7 . The simplest expression (6.25) relates the area of the surface S with the radius squared $\|\vec{r}\|^2$, of the sphere with center on the observation point and tangent to the surface:

$$\Omega = \frac{S}{\|\vec{r}\|^2} \quad (6.25)$$

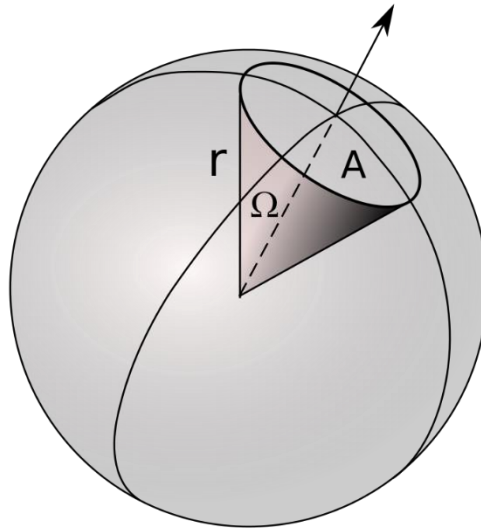


FIGURE 6.7. SOLID ANGLE BY [16]

More accurate results are obtained when integrating the differential of the solid angle, $d\Omega$, (6.26), by differentiating also the surface, dS :

$$d\Omega = \frac{\cos \phi \cdot dS}{\|\vec{r}\|^2} \quad (6.26)$$

In the equation (6.26), ϕ is the angle between the position vector, \vec{r} , and the normal vector of the surface, \vec{n}_π , guaranteeing $\cos \phi \cdot dS$ to be the perpendicular projection of dS to \vec{r} . The cosine of ϕ is calculated as the equation (6.27):

$$\cos \phi = \frac{\vec{n}_\pi \cdot \vec{r}}{\|\vec{n}_\pi\| \cdot \|\vec{r}\|} \quad (6.27)$$

Vector \vec{n}_π , (6.28), is the product of two orthogonal vectors of plane π :

$$\vec{n}_\pi = \vec{v} \times \vec{u} \quad (6.28)$$

Position vector \vec{r} is the difference between the point R contained inside the upper panel plane, obtained like lower panel π_0 by equation (6.5) but considering that the point used to define the plane is the origin of coordinates instead of P_{π_0} in (6.3) and the observation point selected in lower panel P_{π_0f} :

$$\vec{r} = R - P_{\pi_0f} \quad (6.29)$$

$$R = \mu \cdot \vec{v} + \sigma \cdot \vec{u} \quad (6.30)$$

It is important to emphasize that for indirect irradiance model the origin of coordinates is in the axis of symmetry of the upper panel, when in the direct irradiance model, it was on one of the corners.

Summing up the terms, the integration for the surface is presented in (6.31):

$$\Omega = \iint_S \frac{\cos \phi}{\|\vec{r}\|^2} \cdot dS \quad (6.31)$$

If we select the unit normal vector \vec{n}_π ,(6.32),of the surface for the integral rests as shown in expression (6.33):

$$\|\vec{n}_\pi\| = 1 \quad (6.32)$$

$$\Omega = \iint_S \frac{\vec{n}_\pi \cdot \vec{r}}{\|\vec{r}\|^3} \cdot dS \quad (6.33)$$

Finally, introducing the borders of the surface the integral results on (6.34):

$$\Omega = \int_{-\frac{w}{2}}^{\frac{w}{2}} \int_{-\frac{l}{2}}^{\frac{l}{2}} \frac{\vec{n}_\pi \cdot \vec{r}}{\|\vec{r}\|^3} d\sigma d\mu \quad (6.34)$$

For a single panel, more than one observation point is needed to take into consideration the different result depending on the location. The number of points f to divide zones less influenced by indirect shadowing than others depend on the size of the installation. For a single panel modeling, based on the results obtained, it is acceptable to propose three points in order to get the maximum solid angle in the center P_{π_0max} , an intermediate value P_{π_0mid} and the minimum value in the corners P_{π_0min} depicted in (6.35):

$$P_{\pi 0max} = \begin{pmatrix} 0 \\ 0 \\ -h \end{pmatrix} P_{\pi 0mid} = \begin{pmatrix} -L/4 \\ -w/4 \\ -h \end{pmatrix} P_{\pi 0min} = \begin{pmatrix} -L/2 \\ -w/2 \\ -h \end{pmatrix} \quad (6.35)$$

The calculations have been done for a generalist case of a tilted panel and for horizontal panels with some slight changes:

TILTED

The vectors for \vec{v}_t and \vec{u}_t are the same as presented in equations (6.3)(6.4) for plane π_0 :

$$\vec{v}_t = \begin{pmatrix} 0 \\ 1 \\ 0 \end{pmatrix}; \vec{u}_t = \begin{pmatrix} \cos(\beta) \\ 0 \\ \sin(\beta) \end{pmatrix} \quad (6.36)$$

Normal unit vector is obtained by equation(6.28):

$$\vec{n}_{\pi t} = \begin{pmatrix} \sin(\beta) \\ 0 \\ -\cos(\beta) \end{pmatrix} \quad (6.37)$$

Point R corresponding to equation (6.30):

$$R_t = \mu \cdot \begin{pmatrix} 0 \\ 1 \\ 0 \end{pmatrix} + \sigma \cdot \begin{pmatrix} \cos(\beta) \\ 0 \\ \sin(\beta) \end{pmatrix} = \begin{pmatrix} \sigma \cdot \cos(\beta) \\ \mu \\ \sigma \cdot \sin(\beta) \end{pmatrix} \quad (6.38)$$

Position vector, its norm and the integral are calculated for the three points $P_{\pi 0max}$, $P_{\pi 0mid}$ and $P_{\pi 0min}$ following equations (6.29)(6.34):

- $\Omega_{t, P_{\pi 0max}}$

$$\vec{r}_{t, P_{\pi 0max}} = \begin{pmatrix} \sigma \cdot \cos(\beta) \\ \mu \\ \sigma \cdot \sin(\beta) \end{pmatrix} - \begin{pmatrix} 0 \\ 0 \\ -h \end{pmatrix} = \begin{pmatrix} \sigma \cdot \cos(\beta) \\ \mu \\ \sigma \cdot \sin(\beta) + h \end{pmatrix} \quad (6.39)$$

$$\|\vec{r}_{t, P_{\pi 0max}}\| = \sqrt{(\sigma \cdot \cos(\beta))^2 + (\mu)^2 + (\sigma \cdot \sin(\beta) + h)^2} \quad (6.40)$$

$$\Omega_{t,P\pi\text{omax}} = \int_{-\frac{w}{2}}^{\frac{w}{2}} \int_{-\frac{L}{2}}^{\frac{L}{2}} \frac{|-\cos(\beta) \cdot h|}{((\sigma \cdot \cos(\beta))^2 + (\mu)^2 + (\sigma \cdot \sin(\beta) + h)^2)^{\frac{3}{2}}} d\sigma d\mu \quad (6.41)$$

- $\Omega_{t,P\pi\text{omid}}$

$$\|\vec{r}_{t,P\pi\text{omid}}\| = \sqrt{(\sigma \cdot \cos(\beta) + L/4)^2 + (\mu + w/4)^2 + (\sigma \cdot \sin(\beta) + h)^2} \quad (6.42)$$

$$\vec{r}_{t,P\pi\text{omid}} = \begin{pmatrix} \sigma \cdot \cos(\beta) \\ \mu \\ \sigma \cdot \sin(\beta) \end{pmatrix} - \begin{pmatrix} -L/4 \\ -w/4 \\ -h \end{pmatrix} = \begin{pmatrix} \sigma \cdot \cos(\beta) + L/4 \\ \mu + w/4 \\ \sigma \cdot \sin(\beta) + h \end{pmatrix}$$

$$\Omega_{t,P\pi\text{omid}} = \int_{-\frac{w}{2}}^{\frac{w}{2}} \int_{-\frac{L}{2}}^{\frac{L}{2}} \frac{|\sin(\beta) \cdot L/4 - \cos(\beta) \cdot h|}{((\sigma \cdot \cos(\beta) + L/4)^2 + (\mu + w/4)^2 + (\sigma \cdot \sin(\beta) + h)^2)^{\frac{3}{2}}} d\sigma d\mu \quad (6.43)$$

- $\Omega_{t,P\pi\text{omin}}$

$$\vec{r}_{t,P\pi\text{omin}} = \begin{pmatrix} \sigma \cdot \cos(\beta) \\ \mu \\ \sigma \cdot \sin(\beta) \end{pmatrix} - \begin{pmatrix} -L/2 \\ -w/2 \\ -h \end{pmatrix} = \begin{pmatrix} \sigma \cdot \cos(\beta) + L/2 \\ \mu + w/2 \\ \sigma \cdot \sin(\beta) + h \end{pmatrix} \quad (6.44)$$

$$\|\vec{r}_{t,P\pi\text{omin}}\| = \sqrt{(\sigma \cdot \cos(\beta) + L/2)^2 + (\mu + w/2)^2 + (\sigma \cdot \sin(\beta) + h)^2} \quad (6.45)$$

$$\Omega_{t,P\pi\text{omin}} = \int_{-\frac{w}{2}}^{\frac{w}{2}} \int_{-\frac{L}{2}}^{\frac{L}{2}} \frac{|\sin(\beta) \cdot L/2 - \cos(\beta) \cdot h|}{((\sigma \cdot \cos(\beta) + L/2)^2 + (\mu + w/2)^2 + (\sigma \cdot \sin(\beta) + h)^2)^{\frac{3}{2}}} d\sigma d\mu \quad (6.46)$$

The integrals are set in absolute value since the result would be negative by the system of coordinates, but the result would not have physical sense.

HORIZONTAL

For a horizontal case the procedure is the same as applying $\beta=0$ but substituting σ and μ by y and x to propose an integral using the coordinates of the reference system. Again the equations applied are (6.3)(6.4)(6.28)(6.30).

$$\vec{v}_{xy} = \begin{pmatrix} 1 \\ 0 \\ 0 \end{pmatrix}; \vec{u}_{xy} = \begin{pmatrix} 0 \\ 1 \\ 0 \end{pmatrix} \quad (6.47)$$

$$\vec{n}_{\pi,xy} = \begin{pmatrix} 0 \\ 0 \\ 1 \end{pmatrix} \quad (6.48)$$

$$R_{xy} = \mu \cdot \begin{pmatrix} 1 \\ 0 \\ 0 \end{pmatrix} + \sigma \cdot \begin{pmatrix} 0 \\ 1 \\ 0 \end{pmatrix} = x \cdot \begin{pmatrix} 1 \\ 0 \\ 0 \end{pmatrix} + y \cdot \begin{pmatrix} 0 \\ 1 \\ 0 \end{pmatrix} = \begin{pmatrix} x \\ y \\ 0 \end{pmatrix} \quad (6.49)$$

- $\Omega_{xy,P_{\pi\max}}$

$$\vec{r}_{xy,P_{\pi\max}} = \begin{pmatrix} x \\ y \\ 0 \end{pmatrix} - \begin{pmatrix} 0 \\ 0 \\ -h \end{pmatrix} = \begin{pmatrix} x \\ y \\ h \end{pmatrix} \quad (6.50)$$

$$\|\vec{r}_{xy,P_{\pi\max}}\| = \sqrt{x^2 + y^2 + h^2} \quad (6.51)$$

$$\Omega_{xy,P_{\pi\max}} = \int_{-\frac{w}{2}}^{\frac{w}{2}} \int_{-\frac{L}{2}}^{\frac{L}{2}} \frac{h}{(x^2 + y^2 + h^2)^{\frac{3}{2}}} dx dy \quad (6.52)$$

- $\Omega_{xy,P_{\pi\mid\text{id}}}$

$$\vec{r}_{xy,P_{\pi\mid\text{id}}} = \begin{pmatrix} x \\ y \\ 0 \end{pmatrix} - \begin{pmatrix} -L/4 \\ -w/4 \\ -h \end{pmatrix} = \begin{pmatrix} x + L/4 \\ y + w/4 \\ h \end{pmatrix} \quad (6.53)$$

$$\|\vec{r}_{xy,P_{\pi\mid\text{id}}}\| = \sqrt{(x + L/4)^2 + (y + w/4)^2 + h^2} \quad (6.54)$$

$$\Omega_{xy,P_{\pi\mid\text{id}}} = \int_{-\frac{w}{2}}^{\frac{w}{2}} \int_{-\frac{L}{2}}^{\frac{L}{2}} \frac{h}{((x + L/4)^2 + (y + w/4)^2 + h^2)^{\frac{3}{2}}} dx dy \quad (6.55)$$

- $\Omega_{xy,P_{\pi\text{min}}}$

$$\vec{r}_{xy,P_{\pi\text{min}}} = \begin{pmatrix} x \\ y \\ 0 \end{pmatrix} - \begin{pmatrix} -L/2 \\ -w/2 \\ -h \end{pmatrix} = \begin{pmatrix} x + L/2 \\ y + w/2 \\ h \end{pmatrix} \quad (6.56)$$

$$\|\vec{r}_{xy,P_{\pi min}}\| = \sqrt{(x + L/2)^2 + (y + w/2)^2 + h^2} \quad (6.57)$$

$$\Omega_{xy,P_{\pi min}} = \int_{-\frac{w}{2}}^{\frac{w}{2}} \int_{-\frac{L}{2}}^{\frac{L}{2}} \frac{h}{\left((x + L/2)^2 + (y + w/2)^2 + h^2\right)^{\frac{3}{2}}} dx dy \quad (6.58)$$

An additional solid angle is obtained as combination of the f points used to approximate a homogeneous solid angle reduction. In the case of f=3, the equation (6.59) describes the approximation since a 25% of the area is between maximum and medium point and a 75% of the area between medium point and minimum point.

$$\Omega_{j,eq} = \frac{\Omega_{j,P_{\pi max}} - \Omega_{j,P_{\pi mid}}}{2} \cdot 0'25 + \frac{\Omega_{j,P_{\pi mid}} - \Omega_{j,P_{\pi min}}}{2} \cdot 0'75 \quad (6.59)$$

The solid angles put into account are the critical reduction, $\Omega_{j,red_{cr}}$, caused by the biggest obstruction, accomplished in the center of the installation, and the equivalent reduction, $\Omega_{j,red_{eq}}$, for a more permissive criterion.

The proportion of solid angle available is calculated as in equations (6.60)(6.61)

$$\Omega_{j,red_{eq}} = \frac{\Omega_{full} - \Omega_{j,eq}}{\Omega_{full}} \quad (6.60)$$

$$\Omega_{j,red_{cr}} = \frac{\Omega_{full} - \Omega_{j,max}}{\Omega_{full}} \quad (6.61)$$

The amount of diffuse irradiance and irradiation are obtained by equations(6.62)(6.63)(6.64)(6.65)

$$G_{d/mj,red_{eq}} = G_{d/m^2} \cdot \Omega_{j,red_{eq}} \quad (6.62)$$

$$G_{d/mj,red_{cr}} = G_{d/m^2} \cdot \Omega_{j,red_{cr}} \quad (6.63)$$

$$G_{d,j,eq} = G_{d/m^2,j,red_{eq}} \cdot l \cdot w \quad (6.64)$$

$$G_{d,j,cr} = G_{d/m^2,j,red_{cr}} \cdot l \cdot w \quad (6.65)$$

6.2.2 Procedure for indirect irradiance model

The model for indirect irradiance can be programmed in several languages as well but the most sensible choice is using the same as the used for the direct irradiance model, in order to use common variables.

Nonetheless, the integral cannot be calculated on an analytical way so numeric calculations are needed. Several software and programming environments such as Mathematica, MATLAB or Python are suitable for the calculation.

The example proposed has been programmed in Microsoft Excel, using the same file programmed for the direct irradiance example. The integrals have been calculated with MATLAB since is also a very accessible software.

The procedure starts calculating the integrals in equations (6.52)(6.55)(6.58) for the horizontal case and then the ones in equations (6.41)(6.43)(6.46) for a tilted case. If we had $f > 3$ more equations should be described and applied.

This calculation requires a brief script in MATLAB with a loop for Δh configured with the integer function defined as the proper equation of those mentioned. Variables l , w and β for tilting must be declared.

The results for the geometric parameters selected in the example, for tilted and horizontal, and for the points described in equation (6.35) are shown in Table 6.11 and Table 6.12 in sr.

TABLE 6.11. HORIZONTAL SOLID ANGLE

h	Max	mid	min
1	1,18	1,02	0,66
1,25	0,84	0,75	0,53
1,5	0,63	0,57	0,43
1,75	0,48	0,44	0,35
2	0,38	0,36	0,29
2,25	0,31	0,29	0,25
2,5	0,25	0,24	0,21
2,75	0,21	0,20	0,18
3	0,18	0,17	0,16
3,25	0,15	0,15	0,14
3,5	0,13	0,13	0,12

TABLE 6.12. TILTED SOLID ANGLE

h	Max	mid	min
1	1,13	0,80	0,34
1,25	0,79	0,60	0,32
1,5	0,58	0,46	0,28
1,75	0,44	0,36	0,25
2	0,35	0,29	0,21
2,25	0,28	0,24	0,18
2,5	0,23	0,20	0,16
2,75	0,19	0,17	0,14
3	0,16	0,15	0,12
3,25	0,14	0,13	0,11
3,5	0,12	0,11	0,10

The comparison between horizontal and tilted results demonstrates that the difference could be neglected for low β degrees values, considering the example is operated for Wroclaw, which has high latitude and consequently higher β than other areas where solar panels are more profitable.

The equation (6.59) is also applied to obtain the eq angle as in the Table 6.15 and the Table 6.16.

TABLE 6.13. HORIZONTAL EQUIVALENT SOLID ANGLE

h	eq
1	0,90
1,25	0,68
1,5	0,52
1,75	0,41
2	0,34
2,25	0,28
2,5	0,23
2,75	0,20
3	0,17
3,25	0,15
3,5	0,13

TABLE 6.14. TILTED EQUIVALENT SOLID ANGLE

h	eq
1	0,67
1,25	0,52
1,5	0,41
1,75	0,33
2	0,27
2,25	0,22
2,5	0,19
2,75	0,16
3	0,14
3,25	0,12
3,5	0,11

The solid angle available is calculated by equation (6.60)(6.61) and added to the table as in the Table 6.13 and Table 6.14 for the example:

TABLE 6.15. HORIZONTAL AVAILABLE ANGLES

h	Ω_{crit}	Ω_{eq}
1	0,81	0,86
1,25	0,87	0,89
1,5	0,90	0,92
1,75	0,92	0,93
2	0,94	0,95
2,25	0,95	0,96
2,5	0,96	0,96
2,75	0,97	0,97
3	0,97	0,97
3,25	0,98	0,98
3,5	0,98	0,98

TABLE 6.16. TILTED AVAILABLE ANGLES

h	Ω_{crit}	Ω_{eq}
1	0,82	0,89
1,25	0,87	0,92
1,5	0,91	0,93
1,75	0,93	0,95
2	0,94	0,96
2,25	0,96	0,96
2,5	0,96	0,97
2,75	0,97	0,97
3	0,97	0,98
3,25	0,98	0,98
3,5	0,98	0,98

As in chapter 5.1.2 Procedure for direct irradiance model of the report, G_d/m from irradiance data is related with the values of chapter 5 and through equation (6.62)(6.63), $G_{d/m,j,red}$ is obtained for each moment of the year discretized as explained in chapters 4 and 5. Finally, eq (6.64)(6.65) gives the indirect irradiation resultant.

The Table 6.18.Tilted and Table 6.17 represent a fragment of the whole calculation endured in the model example for horizontal and tilted planes, for $h = 1,75$ and $h = 2$, the months of September and October and the panel size selected before.

TABLE 6.17. HORIZONTAL INDIRECT IRRADIANCE & IRRADIATION 10TH OF SEPTEMBER & 10TH OF OCTOBER

	H=1,75					H=2			
	Gd/m	Gd/m crit	Gd/m eq	Gd_crit	Gd_eq	Gd/m crit	Gd/m eq	Gd_crit	Gd_eq
4:00	0	0,00	0,00	0,00	0,00	0,00	0,00	0,00	0,00
5:00	0	0,00	0,00	0,00	0,00	0,00	0,00	0,00	0,00
6:00	23,45	21,65	21,90	36,81	37,24	22,03	22,20	37,45	37,74
7:00	77,49	71,55	72,38	121,64	123,04	72,80	73,35	123,77	124,70
8:00	125,07	115,49	116,82	196,33	198,59	117,51	118,39	199,76	201,27
9:00	163,25	150,75	152,48	256,27	259,22	153,38	154,54	260,74	262,71
10:00	188,85	174,38	176,39	296,45	299,87	177,43	178,77	301,63	303,91
11:00	203,54	187,95	190,11	319,51	323,19	191,23	192,67	325,09	327,55
12:00	207,84	191,92	194,13	326,26	330,02	195,27	196,74	331,96	334,47
13:00	192,88	178,11	180,16	302,78	306,26	181,21	182,58	308,06	310,39
14:00	172,62	159,40	161,23	270,98	274,09	162,18	163,40	275,70	277,79
15:00	134,04	123,77	125,20	210,41	212,84	125,93	126,88	214,09	215,70
16:00	93,9	86,71	87,71	147,40	149,10	88,22	88,89	149,97	151,11
17:00	38,71	35,74	36,16	60,77	61,47	36,37	36,64	61,83	62,29
18:00	1,81	1,67	1,69	2,84	2,87	1,70	1,71	2,89	2,91
19:00	0	0,00	0,00	0,00	0,00	0,00	0,00	0,00	0,00
20:00	0	0,00	0,00	0,00	0,00	0,00	0,00	0,00	0,00
4:00	0	0,00	0,00	0,00	0,00	0,00	0,00	0,00	0,00
5:00	0	0,00	0,00	0,00	0,00	0,00	0,00	0,00	0,00
6:00	0,14	0,13	0,13	0,22	0,22	0,13	0,13	0,22	0,23
7:00	40,65	37,54	37,97	63,81	64,55	38,19	38,48	64,93	65,42
8:00	92,86	85,75	86,73	145,77	147,45	87,24	87,90	148,31	149,43
9:00	132,84	122,66	124,08	208,53	210,93	124,81	125,75	212,17	213,77
10:00	149,85	138,37	139,96	235,23	237,94	140,79	141,85	239,34	241,15
11:00	163,05	150,56	152,29	255,95	258,90	153,19	154,35	260,42	262,39
12:00	159,81	147,57	149,27	250,87	253,75	150,14	151,28	255,24	257,17
13:00	145,71	134,55	136,10	228,73	231,37	136,90	137,93	232,72	234,48
14:00	124,32	114,80	116,12	195,16	197,40	116,80	117,68	198,56	200,06
15:00	87,5	80,80	81,73	137,36	138,94	82,21	82,83	139,75	140,81
16:00	38,58	35,62	36,03	60,56	61,26	36,25	36,52	61,62	62,08
17:00	0,19	0,18	0,18	0,30	0,30	0,18	0,18	0,30	0,31
18:00	0	0,00	0,00	0,00	0,00	0,00	0,00	0,00	0,00
19:00	0	0,00	0,00	0,00	0,00	0,00	0,00	0,00	0,00
20:00	0	0,00	0,00	0,00	0,00	0,00	0,00	0,00	0,00

TABLE 6.18. TILTED INDIRECT IRRADIANCE & IRRADIATION 10TH OF SEPTEMBER & 10TH OF OCTOBER

	H=1,75					H=2			
	Gd/m	Gd/m crit	Gd/m eq	Gd_crit	Gd_eq	Gd/m crit	Gd/m eq	Gd_crit	Gd_eq
4:00	0	0,00	0,00	0,00	0,00	0,00	0,00	0,00	0,00
5:00	0	0,00	0,00	0,00	0,00	0,00	0,00	0,00	0,00
6:00	23,45	21,79	22,22	37,05	37,77	22,15	22,44	37,66	38,15
7:00	77,49	72,02	73,42	122,43	124,82	73,20	74,16	124,44	126,08
8:00	125,07	116,24	118,51	197,61	201,47	118,14	119,70	200,85	203,49
9:00	163,25	151,73	154,69	257,93	262,97	154,21	156,24	262,16	265,61
10:00	188,85	175,52	178,94	298,38	304,20	178,39	180,74	303,27	307,26
11:00	203,54	189,17	192,86	321,59	327,87	192,27	194,80	326,86	331,16
12:00	207,84	193,17	196,94	328,39	334,79	196,33	198,92	333,76	338,16
13:00	192,88	179,26	182,76	304,75	310,69	182,20	184,60	309,74	313,82
14:00	172,62	160,43	163,56	272,74	278,06	163,06	165,21	277,21	280,86
15:00	134,04	124,58	127,01	211,78	215,91	126,62	128,29	215,25	218,09
16:00	93,9	87,27	88,97	148,36	151,26	88,70	89,87	150,79	152,78
17:00	38,71	35,98	36,68	61,16	62,35	36,57	37,05	62,16	62,98
18:00	1,81	1,68	1,72	2,86	2,92	1,71	1,73	2,91	2,94
19:00	0	0,00	0,00	0,00	0,00	0,00	0,00	0,00	0,00
20:00	0	0,00	0,00	0,00	0,00	0,00	0,00	0,00	0,00
4:00	0	0,00	0,00	0,00	0,00	0,00	0,00	0,00	0,00
5:00	0	0,00	0,00	0,00	0,00	0,00	0,00	0,00	0,00
6:00	0,14	0,13	0,13	0,22	0,23	0,13	0,13	0,22	0,23
7:00	40,65	37,78	38,52	64,23	65,48	38,40	38,91	65,28	66,14
8:00	92,86	86,31	87,99	146,72	149,58	87,72	88,87	149,12	151,09
9:00	132,84	123,46	125,87	209,89	213,98	125,48	127,14	213,32	216,13
10:00	149,85	139,27	141,99	236,76	241,38	141,55	143,42	240,64	243,81
11:00	163,05	151,54	154,50	257,62	262,64	154,02	156,05	261,84	265,29
12:00	159,81	148,53	151,43	252,50	257,43	150,96	152,95	256,63	260,01
13:00	145,71	135,42	138,07	230,22	234,71	137,64	139,46	233,99	237,07
14:00	124,32	115,54	117,80	196,43	200,26	117,44	118,98	199,64	202,27
15:00	87,5	81,32	82,91	138,25	140,95	82,66	83,74	140,51	142,36
16:00	38,58	35,86	36,56	60,96	62,15	36,44	36,92	61,95	62,77
17:00	0,19	0,18	0,18	0,30	0,31	0,18	0,18	0,31	0,31
18:00	0	0,00	0,00	0,00	0,00	0,00	0,00	0,00	0,00
19:00	0	0,00	0,00	0,00	0,00	0,00	0,00	0,00	0,00
20:00	0	0,00	0,00	0,00	0,00	0,00	0,00	0,00	0,00

6.3 Model for Global Irradiance.

The previous chapters 6.1 and 6.2 described with accuracy the behavior of the shadow over the panel. There is plenty of useful data obtained by the model, in this project the results given will be the raw energy income received with the shadowing conditions, but the individual irradiation data for each hour discretized could be also a useful result for further analysis based on the model.

The irradiations obtained can be summed up and compared with the irradiation of a non-shadowed panel calculated as (6.67) to evaluate the efficiency of the distribution.

Equation (6.66) provide the total energy received by the panel, assuming uniform irradiation per hour and for $j = eq$ or cr , in $[kWh]$:

$$G_{year} = \sum G_b + \sum G_{d,j} \quad (6.66)$$

The efficiency ε_{shade} is set as equation (6.68):

$$G_{year_max} = \sum(G_{\frac{b}{m^2}} \cdot w \cdot l) + \sum(G_{\frac{d}{m^2}} \cdot w \cdot l) \quad (6.67)$$

$$\varepsilon_{shade} = \frac{G_{year}}{G_{year_max}} \quad (6.68)$$

The single panel distribution in Wroclaw used as example provides the following results in Table 6.19. Results for G_{eq} and Table 6.20 :

TABLE 6.19. RESULTS FOR G_{EQ}

Direct				Indirect				Global			
h	kWh/year	eff	%	h	kWh/year	eff	%	h	kWh/year	eff	%
1	32,25	73,80	%	1	26,55	89,31	%	1	58,80	80,08	%
1,25	35,91	82,16	%	1,25	27,27	91,73	%	1,25	63,18	86,03	%
1,5	38,47	88,03	%	1,5	27,79	93,48	%	1,5	66,26	90,24	%
1,75	40,12	91,81	%	1,75	27,77	93,40	%	1,75	67,89	92,45	%
2	41,23	94,34	%	2	28,14	94,66	%	2	69,37	94,47	%
2,25	42,06	96,24	%	2,25	28,42	95,60	%	2,25	70,48	95,98	%
2,5	42,73	97,78	%	2,5	28,63	96,32	%	2,5	71,37	97,19	%
2,75	43,12	98,67	%	2,75	28,80	96,89	%	2,75	71,93	97,95	%
3	43,42	99,34	%	3	28,93	97,33	%	3	72,35	98,53	%
3,25	43,59	99,74	%	3,25	29,04	97,69	%	3,25	72,63	98,91	%
3,5	43,70	100,00	%	3,5	29,10	97,87	%	3,5	72,80	99,14	%
				max	29,73	100,00	%				

TABLE 6.20. RESULTS FOR G_CR

Direct				Indirect				Global			
h	kWh/year	eff	%	h	kWh/year	eff	%	h	kWh/year	eff	%
1	32,25	73,80	%	1	24,39	82,04	%	1	56,64	77,13	%
1,25	35,91	82,16	%	1,25	25,98	87,38	%	1,25	61,88	84,27	%
1,5	38,47	88,03	%	1,5	26,97	90,73	%	1,5	65,45	89,13	%
1,75	40,12	91,81	%	1,75	27,45	92,34	%	1,75	67,57	92,02	%
2	41,23	94,34	%	2	27,93	93,95	%	2	69,16	94,18	%
2,25	42,06	96,24	%	2,25	28,28	95,11	%	2,25	70,33	95,78	%
2,5	42,73	97,78	%	2,5	28,53	95,98	%	2,5	71,27	97,05	%
2,75	43,12	98,67	%	2,75	28,73	96,64	%	2,75	71,85	97,85	%
3	43,42	99,34	%	3	28,88	97,15	%	3	72,30	98,45	%
3,25	43,59	99,74	%	3,25	29,00	97,55	%	3,25	72,59	98,85	%
3,5	43,70	100,00	%	3,5	29,10	97,87	%	3,5	72,80	99,14	%
				max	29,73	100,00	%				

The difference shown in Figure 6.8 between both efficiencies can be considered at lower h values but negligible as the shadowing impact decreases

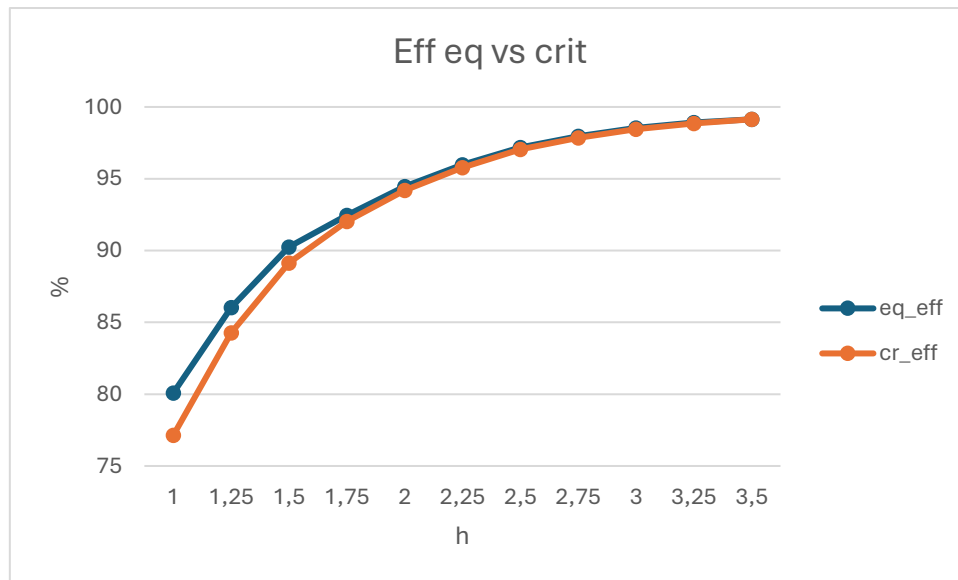


FIGURE 6.8. EFFICIENCY COMPARISON

The Figure 6.9 sums up the execution of the whole model:

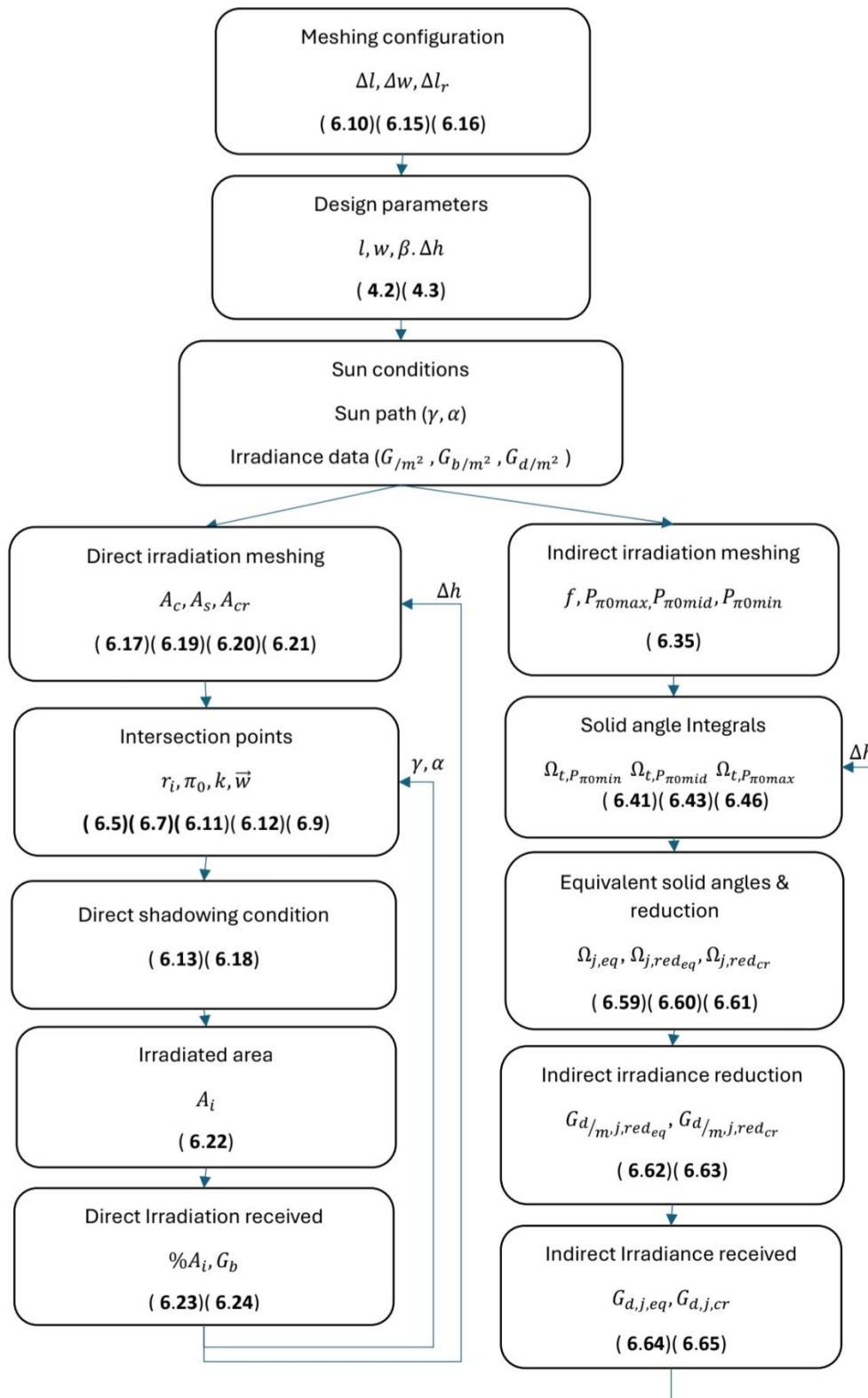


FIGURE 6.9. BLOCK DIAGRAM

7. Conclusions

The study presented combines physical and astronomical information with geometrical basis to model the shadowing phenomenon obtaining reasonable results.

The main conclusion is showed in Figure 6.8 where we can see that the distance between panels h has a direct influence on the power production of the panels, around a 20% for the given example and, since the solid angle occupied would be much higher in bigger installations and the direct radiation rays follow a side-to-side leaned trajectory, for installations with more panels aligned would see this reduction impact even more.

Also, the Figure 6.8 illustrates that there is a difference between considering the most unfavorable point for indirect irradiation and approximating it with more points. The difference is not relevant for a single panel but since the model takes it into consideration, (Volker Quaschnig, 1988) a higher difference for more complex installations would not be incorrectly neglected using this methodology.

It can be stated also that based on Table 6.19 and Table 6.20 the impact of shadowing in a single panel is not extremely significant to the global efficiency of the installation. This result is explained by several reasons.

Firstly, the main factor that provides such optimistic results is the fact that for the direct irradiation model each sector has been considered independent from the others. Real photovoltaic panels have their cells connected in series and, if irradiance falls behind $100 \frac{kW}{m^2}$, the photodiode on the cell will cease to conduct, blocking part of panel production and causing damage to the device. Normalized panels usually possess three independent modules with bypass diodes in parallel to prevent major malfunctions. Therefore, more realistic approaches of modeling should include that whenever some part of the panel is shaded, the reduced indirect irradiance must be over the said limit to avoid production interruption of a third of panel area.

Secondly, the example for the module is forced to discretize the surface and consequently the values are less precise for lower Δl , Δw , Δl_r and specially f for indirect irradiance.

Thirdly, it was expected to obtain nearly negligible energy reduction for a single panel since smaller dimensions produce less intersections between the cast of the shadow and a reduced surface blocking the solid angle available.

Despite that approximation for the results, the model developed behaves with coherence and provides relatively accurate tracking of direct shadowing, with around ten thousand data values obtained in seconds after programming, serving as the ground basis for more complex models and specific modulation of commercial panels.

For those reasons, it can be stated that the model folds a handful method to determine the energetic reduction in vertical distributed PV installations, with a wide versatility among a considerable number of generalized variables and can be easily applied to specific situations without needing powerful software.

8. References

- [1]. https://re.jrc.ec.europa.eu/pvg_tools/en/#TMY
- [2].
- [3]. ABB Group. (2011). Producción energética. In A. Group, *Cuaderno de aplicaciones técnicas n.º 10* (pp. 18-22).
- [4]. Brian Goss, I. C. (2014). Irradiance modelling for individual cells of shaded solar photovoltaic arrays. In *Solar Energy, Volume 110* (pp. 410-419).
- [5]. Volker Quaschnig, R. H. (1988). Irradiance calculation on shaded surfaces. In *Solar Energy, Volume 62, Issue 5* (pp. 369-375).
- [6]. <https://rammb.cira.colostate.edu/wmovl/vrl/tutorials/euromet/courses/spanish/satmet/s2710/s2710006.htm>
- [7]. <https://www.sciencedirect.com/topics/engineering/solar-declination#:~:text=The%20earth's%20axis%20results%20in,%2C%20with%20January%201%20%2B%201.>
- [8]. <https://www.gaisma.com/en/location/wroclaw.html>
- [9]. <https://mastersinsolar.es/base-de-conocimiento/blog-energia-solar/influencia-de-las-sombras/>
- [10]. https://mathinsight.org/double_integral_area
- [11]. <https://www.imagecircuits.com/rb/sunpath.htm>
- [12]. <https://www.magneticdeclination.com/Poland/Wroc%C3%85%E2%80%9Aaw/2124621.html>
- [13]. <https://steemit.com/stem-espanol/@tsoldovieri/angulo-solido-subtendido-por-una-placa-rectangular-con-respecto-a-un-punto-situado-en-su-eje-de-simetria>
- [14]. <https://physics.weber.edu/schroeder/ua/SunAndSeasons.html>
- [15]. <https://mathworld.wolfram.com/SolidAngle.html>
- [16]. <https://www.planete-energies.com/en/media/article/growth-photovoltaic-solar-power-around-world>
- [17]. https://en.wikipedia.org/wiki/Solid_angle